J Mater Sci (2014) 49:1150–1156
DOI 10.1007/s10853-013-7794-7

Hardness and fracture toughness of thermoelectric $La_{3-x}Te_4$

James M. Ma · Samad A. Firdosy · Richard B. Kaner · Jean-Pierre Fleurial · Vilupanur A. Ravi

Received: 13 July 2013 / Accepted: 1 October 2013 / Published online: 22 October 2013

Abstract Lanthanum telluride ($La_{3-x}Te_4$) is a state-of-the-art *n*-type high temperature thermoelectric material that behaves as a weak and brittle ceramic. Vickers microindentation hardness testing was explored as a rapid analysis technique to characterize the mechanical properties of this material. An indentation size effect was observed with hardness values ranging from 439 ± 31 kgf/mm^2 (0.01 kgf/10 s contact time) to 335 ± 6 kgf/mm^2 (0.5 kgf/10 s contact time). The Vickers indentation fracture toughness, K_{VIF}, based on measurements of crack lengths emanating from the corners of the Vickers indents was 0.70 ± 0.06 MPa m$^{1/2}$.

Introduction

Thermoelectric generators have a proven record of reliability in space applications with >30 years of continuous service as implemented in the Voyager 1 and 2 missions. Recent advances in materials research have led to higher efficiency materials with roughly a twofold improvement in energy conversion efficiency over legacy materials such as $Si_{1-x}Ge_x$ and PbTe [1–3]. A significant challenge in developing these new high-efficiency materials into functional devices has been that several of these materials, such as $La_{3-x}Te_4$, behave as weak and brittle ceramics. The fragility of these materials increases the complexity of machining, lowers the yield, and constrains potential device configurations. All of these factors add to the cost and difficulties in developing functional devices.

Efforts are underway to optimize processing conditions and to develop a new class of high-strength high-efficiency materials for use in advanced thermoelectric devices. However, a baseline understanding of mechanical behavior is necessary for comparisons to be made effectively. Furthermore, fast and reliable means to correlate mechanical behavior to process and composition changes are important to be able to assess progress toward this goal.

Although routinely done for engineering ceramics, the challenges in obtaining mechanical property data for thermoelectric materials are significant because they are weak, brittle, air and water sensitive, and expensive. As a result, for many thermoelectric materials it is difficult to machine specimens into geometries required by standardized testing protocols, such as those prescribed for obtaining fracture toughness (K_{IC}) [4, 5] and flexural strength [6, 7], by ASTM International (formerly known as the American Society for Testing and Materials, ASTM), etc. In addition, the stochastic nature of brittle failures requires testing $n \geq 30$ flexural samples to obtain the Weibull parameters and $n \geq 4$ for fracture toughness from Chevron V-notched beam (CVNB) or single-edge-notched beam testing procedures.

Difficulties in preparing samples of sufficient quality have limited the investigation of fracture toughness to a handful of thermoelectric materials such as skutterudites,

J. M. Ma · S. A. Firdosy · J.-P. Fleurial · V. A. Ravi (✉)
Jet Propulsion Laboratory, California Institute of Technology, Pasadena, CA 91109, USA
e-mail: vravi@csupomona.edu

J. M. Ma · R. B. Kaner
Department of Materials Science and Engineering, University of California, Los Angeles, CA 90095, USA

R. B. Kaner
Department of Chemistry and Biochemistry, University of California, Los Angeles, CA 90095, USA

V. A. Ravi
Department of Chemical and Materials Engineering, California State Polytechnic University, Pomona, CA 91768, USA

Zn_4Sb_3, and SiGe [8–14]. The challenge of sample preparation is not unique to thermoelectric materials and has been addressed for other brittle ceramic materials with correlation models developed over the past 50+ years, which relate K_{IC} to the surface cracks emanating from the corners during Vickers microindentation hardness testing [6, 15–25].

Hardness testing stands out as an ideal method to provide information on mechanical properties because it is nondestructive, fast, inexpensive, and requires only limited sample sizes. In addition, the hardness of a material is a complex parameter that is sensitive to the chemical composition, grain size, grain shape, porosity, etc. [26]. Although difficult to de-convolute, the hardness value is a measure of many complex phenomena which interact to give rise to mechanical behavior, and therefore can be applied as a useful parameter for assessing mechanical behavior.

Empirically determined correlation equations have been developed for many engineering ceramics relating fracture toughness values obtained through procedures outlined by ASTM E 1820 standard test method for measurement of fracture toughness, to values calculated from the measurement of crack lengths emanating from the corners of Vickers indentations in brittle materials [6, 15–25, 27]. These correlations have proven useful in obtaining good estimates of fracture toughness values in cases where it is difficult to produce acceptable fracture toughness specimens, a situation relevant to thermoelectric materials [28, 29]. In this study, Vickers hardness testing was used to analyze the mechanical characteristics of $La_{3-x}Te_4$. This thermoelectric material is of current significant interest because it has the highest reported efficiency at 1000 °C for a bulk *n*-type material [30]. Hardness and Vickers indentation fracture toughness have been studied as a function of load as a means to evaluate the mechanical behavior of $La_{3-x}Te_4$.

Experimental methods

$La_{3-x}Te_4$ was synthesized using powder metallurgical methods first described by May et al. [30]. Stoichiometric amounts of the elements with a nominal composition of $x = 0.23$ were ball milled and followed by hot-pressing to obtain pellets of >98 % of theoretical density. Test samples were typically 12.7 mm diameter × 1.5 mm thick and were cold-mounted in epoxy. The test specimens were polished flat and parallel to ±0.01 mm. A total of $N = 6$ samples were metallographically ground and diamond polished using different grit sizes (three samples were finished with 1 μm, two with 0.25 μm, and one with 0.01 μm) to examine if hardness or fracture toughness values were affected by the surface finish. Polishing was accomplished using an oil-based lubricant as $La_{3-x}Te_4$ is water reactive.

Vickers indentation hardness values were measured using an Instron Wilson Hardness Tukon T2100B instrument with a maximum 1 kgf load cell. Best practices as outlined by ASTM C 1327-08 standard test method for Vickers indentation hardness of advanced ceramics were followed for measuring the hardness values of these materials [13]. Optical microscope measurements were carried out under ambient conditions immediately after indentation to minimize the possibility of environmentally assisted crack growth. A series of $N_i = 5$ indentations were made for each applied load with a contact time of 10 s for $N = 6$ samples produced under identical processing conditions except for the final surface finish. Grain boundary etching was achieve by soaking a sample polished to a 1-μm diamond finish in a 3 vol% Br_2:MeOH solution for 5 min. Samples were examined using a FEI Nova 600 scanning electron microscope (SEM).

Results and discussion

Grain size determination

Grain size determination was done by using SEM to image a chemically etched surface of highly polished $La_{3-x}Te_4$. A series of five images were analyzed using the linear intercept technique and a representative image of the etched surface is shown in Fig. 1. The ASTM grain size number determined from the average of the 5 measurements was 16.8 [31]. The grain morphology exhibited a distribution of sizes and each grain appeared regular in shape with no observed elongated grains. There was little visible surface porosity which agrees with the high measured geometric density for these samples.

Vickers hardness

The average hardness values of $La_{3-x}Te_4$ are plotted in Fig. 2 with error bars of one standard deviation indicated. The average hardness for all samples is represented by the solid line and is the average of 30 indents for each load. The subgroups for samples with surface finishes of 1, 0.25, and 0.01 μm are also shown in this figure. The % difference between the mean hardness values (compared between 1 and 0.1 μm surface finish and the 1 and 0.25 μm surface finish samples) was predominantly <5 %, a number consistent with the reproducibility estimates cited in ASTMC 1327-08 [34], thereby justifying taking a global average of hardness values over all the surface finishes used in this study. Therefore, the average of the $N = 6$

indents is representative of the hardness of $La_{3-x}Te_4$, i.e., a hardness of HV 439 ± 30 kgf/mm^2 at low loads (0.01 kgf) and a hardness of 335 kgf/mm^2 at high loads (0.5 kgf).

Optical micrograph images of an indent at each load are shown at the top of the plot. The hardness was measured by determining the position of each corner of the indent to obtain the length of the diagonals for the square indent. The larger error bars at low loads occur as a result of difficulties in accurately measuring the small indentations with an optical microscope. The Vickers hardness was calculated by the equation:

$$\mathrm{HV} = \frac{2F\sin\frac{136^\circ}{2}}{d^2} \quad (1)$$

where HV is the Vickers Hardness in kg/mm^2, F is the applied load in kgf, and d is the length of the diagonal in mm. Since d is small for low loads, the error in measurement Δd becomes more significant. Errors in measurement at low loads can be reduced through measurement with a SEM, but this was found to be unnecessary given the limited usefulness of the low load data and the added complexity of the measurement [32].

$La_{3-x}Te_4$ is a defect compound with the cubic Th_3P_4 crystal structure [33]. The vacancies in the system control the carrier concentration of the material and the thermoelectric performance [30]. The thermoelectric properties of the material are isotropic and the hardness is expected to be as well because the crystal structure is cubic and the samples were synthesized by hot pressing randomly oriented particles. While the hardness may vary as a function of vacancy content, this was beyond the scope of this study. Samples only of thermoelectric interest were studied at the optimized carrier concentration achieved with a vacancy content of $x = 0.23$.

The $La_{3-x}Te_4$ material exhibited crack formation initially at 0.05 kgf and an example of cracking from the Vickers indent is shown in Fig. 3. The length of the crack is denoted by "l" in the image and is measured as a straight line starting from the corner of the indent. As evident in the micrographs shown in Figs. 2 and 3, there is pullout and porosity on the surface of the sample which is common for hard and brittle materials. With reduced polishing it is possible to obtain a surface with fewer pullout voids, but with an increased number of scratches. However, as pointed out before, the differences in hardness values between the different surface finishes were small and within acceptable limits of experimental error.

It was observed that the material exhibited a critical load of 0.5 kgf where spalling, as shown in Fig. 4, occurs and limits the ability to obtain accurate hardness measurements. Tests beyond this load were excluded in accordance with ASTM C1327-08 [34]. Vickers hardness values for $La_{3-x}Te_4$ were measured up to 0.5 kgf, where the values approached a plateau of HV = 335 ± 6 kgf/mm^2 (0.5 kgf/10 s contact). In comparison, $La_{3-x}Te_4$ is soft relative to silicon carbide, a structural ceramic which has a hardness value of HV of ~2500 kgf/mm^2 [15] and was closer to glass with an HV of ~500–1000 kgf/mm^2. Materials with higher hardness values would be more resistant to surface defects during handling and operation, thus reducing the number of potentially fatal defects. However, $La_{3-x}Te_4$ was not a particularly hard ceramic and was observed to be brittle, thus reflecting the challenges of working with this particular material.

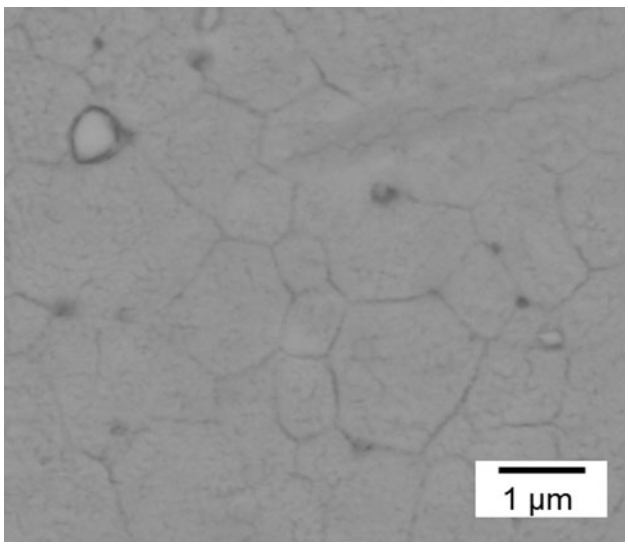

Fig. 1 Backscattered electron image of a chemically etched $La_{3-x}Te_4$ surface. The ASTM grain size was determined to be 16.8 through the linear intercept technique

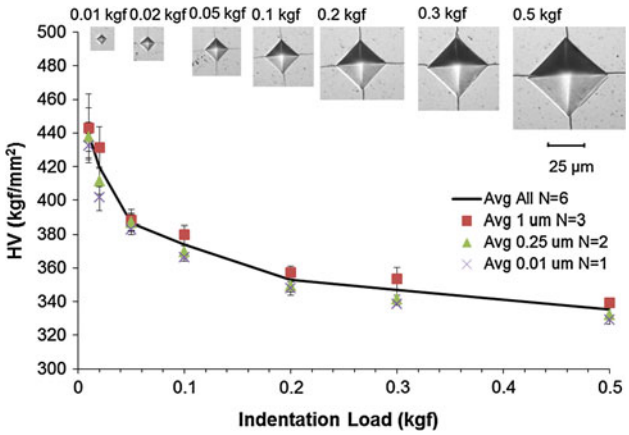

Fig. 2 Average Vickers hardness values as a function of applied load for $La_{3-x}Te_4$. The solid line represents an average of all surface finishes for $N = 6$ samples and $N_i = 5$ indents per sample per applied load. The optical microscope images of samples polished using 0.25-μm diamond paste are provided along the top of the graph (all images are at the same magnification). Spalling occurred above 0.5 kgf so measurements attempted at 1 kgf have been excluded. *Error bars* represent 1 standard deviation

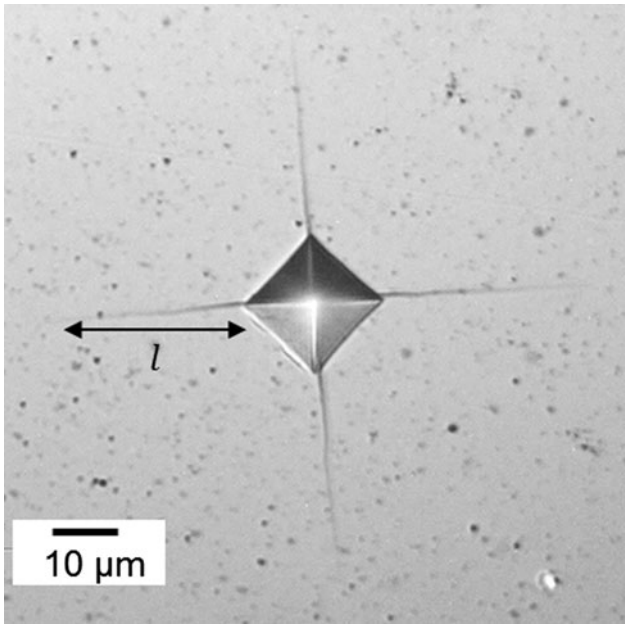

Fig. 3 Optical micrograph of a Vickers indent on $La_{3-x}Te_4$ with a 0.25-μm surface finish. The indent was made under an applied load of 0.1 kgf. Cracks emanating from the corners of the indents were measured to calculate the fracture toughness. The *dark voids* are due to sample pullout and porosity

In comparison to other thermoelectric materials, $La_{3-x}Te_4$ is harder than Bi_2Te_3 HV = 63 kgf/mm^2 [28], silver and antimony-doped PbTe at 0.3 kgf HV = 60–70 kgf/mm^2 [35], and PbTe at 0.01 kgf HV = 24 kgf/mm^2 [36]. It is comparable or slightly softer than the skutterudite class of compounds at 0.1 kgf HV = 250–550 kgf/mm^2 which varies depending on the specific composition [37]. The lanthanum telluride hardness values reported here are significantly lower than those reported for $Si_{0.8}Ge_{0.2}$ (1264–1499 kgf/mm^2) [38].

$La_{3-x}Te_4$ exhibited a Vickers hardness indentation size effect (ISE), i.e., higher hardness values at lower indentation loads, a phenomenon that has been reported in microhardness testing for a wide range of metallic and ceramic materials [39]. Although there remains some controversy about the origin of the ISE effect, the reader is referred to the following review papers for additional information [40–45]. Ideally, hardness values should be load-independent (e.g., at high loads) or at least have the testing load specified to ensure proper comparison between materials systems. For $La_{3-x}Te_4$, the hardness value approaches ~340 kgf/mm^2 at the spalling limit and can be used as a basis for comparison. It has been previously reported that the brittleness of a material is inversely proportional to the load at which the onset of cracking occurs during indentation [46]. Therefore, rather than analyzing and reporting single load hardness values, it is useful that hardness testing be conducted at multiple loads to gain deeper insights into the mechanical behavior of thermoelectric materials.

For $La_{3-x}Te_4$, the onset of cracking was detected using the optical microscope at 0.05 kgf (although finer cracks have been detected at loads as low as 0.02 kgf using the SEM) and correlates well with the region of sharply decreasing hardness values as seen in Fig. 2. This early onset of cracking indicates that the material is fairly brittle. However, due to instrument limitations in indentation load step sizes, it was not possible to probe the samples at a sufficiently high resolution to determine the critical loads for the onset of crack formation. Nevertheless, these results agree with the observed apparent brittleness of $La_{3-x}Te_4$

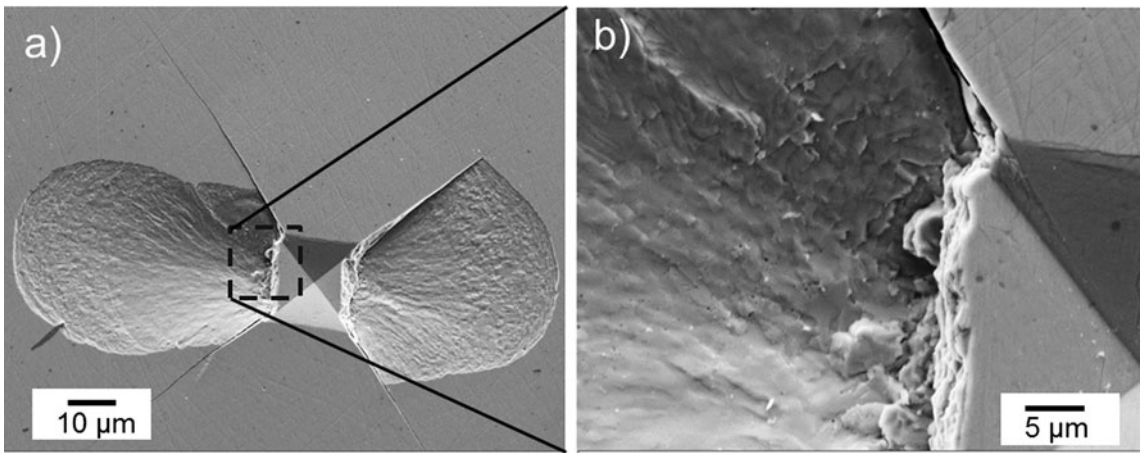

Fig. 4 **a** Scanning electron micrograph of a Vickers indent made under a load of 1.0 kgf. Spalling was observed to the *left* and the *right* of the indent image. This load corresponds with the transition from the Palmqvist regime of surface cracks to the half-penny regime which is a mixture of surface and radial cracks. The roughness of the fractured surface at the points furthest from the indent is indicative of intergranular fracture following grain boundaries. **b** A magnified view of where the indent meets the spalled surface. The smoothness of the fracture surface is mirror like and is indicative of transgranular fracture across grain boundaries

observed during machining and handling of the material. $La_{3-x}Te_4$ follows a trend common for ionically bonded polycrystalline materials such that they tend to be brittle. Ionic bonding is generally rigid and resistant to plastic deformation resulting in brittle fracture as the dominate fracture mode [41]. The spalled surface shown in Fig. 4a reflects a mixture of transgranular and intergranular fracture. A magnified view of the spalled surface is shown in Fig. 4b. The region adjacent to the indent shows that the fractured surface is smooth and mirror-like which is characteristic of transgranular fracture. Further away from the indent, the surface exhibits a coarse texture and the roughness of the spalled area is likely due to the crack path following the texture of the grain boundaries. This trend reflects the mirror–mist behavior for brittle ceramics with the transition occurring as the crack velocity decreases away from the origin of failure [47]. With the limited viewing angles into the cracks emanating from the corners of the Vickers indents, it is difficult to identify the exact nature of the fracture for the cracks. However, since the spalling is related to the propagation of the cracks, it is plausible that the cracks follow the same mixed transgranular to intergranular behavior as the cracks extend further from the corner of the indent.

Vickers indentation fracture toughness

Although issues have been raised concerning the accuracy and validity of using empirically derived correlation equations to calculate fracture toughness from Vickers indentation testing [48], the calculated fracture toughness values were approximations, given the sample preparation difficulties in ASTM techniques. A review of the technique by Ponton and Rawlings suggests that the technique is a good approximation to within ~30 % for unknown materials and serves as a rapid and convenient measurement technique when fabrication of ASTM test specimens is not possible [32, 49]. Efforts are underway to enhance processing and machining capabilities to produce suitable ASTM materials, but given the current lack of capabilities to produce samples of suitable quality and the need for faster turnaround on mechanical properties, this technique is useful to provide semi-empirical data.

After considering nineteen different methods of analysis, Ponton and Rawlings [32] selected the equation developed by Shetty et al. [24] for materials which exhibit cracking in the Palmqvist regime approximately $l/a \leq 3$:

$$K_c = \frac{1}{3(1-\upsilon^2)(2^{1/2}\pi^{5/2}\tan\theta)}\left(\frac{H_v P}{4l}\right)^{1/2} \quad (2)$$

where υ is the Poisson ratio, θ is the indenter contact angle, H_v is the hardness at load P, a is the length of the 1/2 diagonal of the indent, and l is the edge crack length. The measured l/a for $La_{3-x}Te_4$ ranged from 1.6 to 3 with the value increasing with increasing load. The spalling in the material corresponds well with the transition from Palmqvist surface cracks to the half-penny median radial crack regime $l/a > 3$. Ponton and Rawlings generalized the equation by taking $\upsilon = 0.25$, which is a good approximation for brittle materials, and $\theta = 68°$ for a Vickers indent

$$K_C = 0.0319\frac{P}{al^{1/2}} \quad (3)$$

Crack lengths for loads ranging from 0.05 to 0.5 kgf were measured and are shown in Fig. 5. As noted before, errors in measurements at low loads arise due to difficulties in measuring small crack lengths using an optical microscope. At high loads, the tortuous nature of the crack paths leads to errors in crack length measurements. The crack lengths as a function of load follow a linear relationship with $R^2 = 0.9965$. The linear relationship between crack length and indent load was also observed by Shetty, Wright, Mincer, and Clauer in WC–Co cermets [24].

The calculated Vickers indentation fracture toughness is reported in Fig. 6. The values exhibit a subtle variation with $K_{VIF} = 0.68 \pm 0.17$ MPa $m^{1/2}$ at low loads (0.05 kgf) to 0.71 ± 0.06 MPa $m^{1/2}$ at high loads (0.5 kgf). The minimum dispersion in the data was observed at 0.3 kgf with $K_{VIF} = 0.70 \pm 0.06$ MPa $m^{1/2}$. The lower error corresponds to a balance between the indent being sufficiently large, exhibiting long crack formation, and ideal linear crack formation. The cracks and indents at lower loads were difficult to measure using the optical microscope and at 0.5 kgf there was a breakdown from the idealized crack formation with crack branching and nonlinear cracks. Similar to the Vickers hardness, the observed differences in fracture toughness as a function of

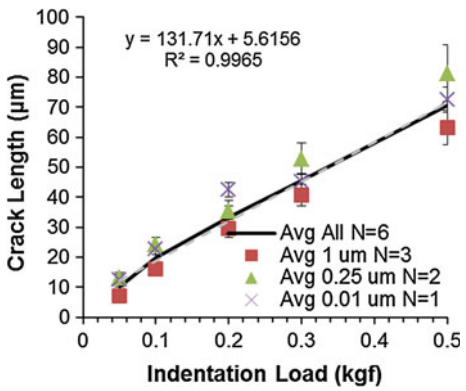

Fig. 5 Average crack lengths for indentation loads between 0.05 and 0.5 kgf. No cracks were detected below 0.05 kgf using an optical microscope. *Error bars* represent 1 standard deviation

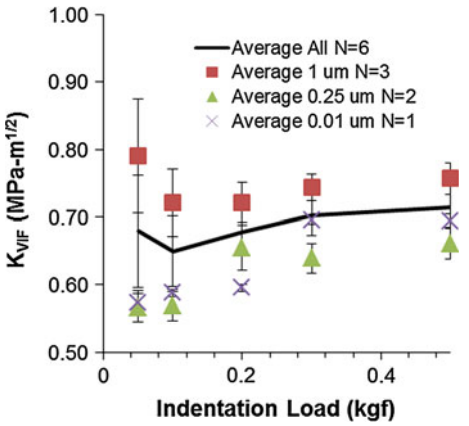

Fig. 6 Vickers indentation fracture toughness K_{VIF} calculated from the measured crack lengths produced by Vickers indentations for $La_{3-x}Te_4$. No variation greater than the error measurement of K_{VIF} was observed as a function of surface finish within the limits of experimental uncertainty and the uncertainty of the correlation model. *Error bars* represent 1 standard deviation

surface finish were within the limits of experimental error and the uncertainty of the SWMC model.

The calculated fracture toughness corresponds well to the qualitatively observed brittle behavior of these materials. It is interesting to note that this value is comparable to the fracture toughness (K_{Ic}) of soda lime glass $K_{IC} = 0.7$ MPa $m^{1/2}$ as measured through traditional techniques [50]. $La_{3-x}Te_4$ is more brittle when compared to other thermoelectric materials such as different compositions of the skutterudite class of thermoelectric materials that have fracture toughnesses of $K_{IC} = 1.1$–2.8 MPa $m^{1/2}$ as determined by the CVNB test [13], and $K_{VIF} = 1.5$–2.2 MPa $m^{1/2}$ [37]. Bismuth telluride, Bi_2Te_3, also has a higher fracture toughness compared to $La_{3-x}Te_4$ with K_{VIF} values of 1.14 MPa $m^{1/2}$ [28]. However, $La_{3-x}Te_4$ is not as brittle as the PbTe–PbS materials with a reported K_{VIF} of 0.35 MPa $m^{1/2}$ [51].

It is important to realize that at this stage of development it is very difficult to obtain samples of advanced thermoelectric materials which will satisfy ASTM specifications. Furthermore, these insights have allowed us to devise novel methods to obtain materials with enhanced mechanical behavior, thereby making this technique a useful tool for process optimization for a given material, as well as for comparisons between different classes of materials.

Conclusion

The Vickers hardness values have been measured for $La_{3-x}Te_4$ as a function of applied load. The ISE effect is observed for this material and provides important information as to the brittleness of $La_{3-x}Te_4$. From crack measurements of the Vickers indents, the material possesses a fracture toughness value that reflects its brittle glass-like behavior. These values correlate with observations made from machining $La_{3-x}Te_4$ and suggest that the Vickers indentation technique is a useful tool in rapidly characterizing mechanical behavior. Although traditional ASTM K_{IC} techniques are advisable when possible, obtaining an approximate value through Vickers microindentation is useful and represents a practical balance considering the limitations in sample preparation for weak and brittle materials.

Acknowledgements The authors would like to thank Mr. Kevin Smith for experimental assistance and Dr. Sabah K. Bux for helpful discussions. This research was carried out at the Jet Propulsion Laboratory, California Institute of Technology, under a contract with the National Aeronautics and Space Administration. This work was supported by the NASA Science Mission Directorate's Radioisotope Power Systems Technology Advancement Program, the NSF IGERT: Materials Creation Training Program (MCTP) – DGE-0654431, and the California NanoSystems Institute.

References

1. Yang J, Caillat T (2006) MRS Bull J 31:224
2. Fleurial J-P (2009) J Manag 61:79. doi:10.1007/s11837-009-0057-z
3. Snyder GJ, Toberer ES (2008) Nat Mater 7:105
4. ASTM (2010) ASTM Standard, ASTM C1421 - 10 standard test methods for determination of fracture toughness of advanced ceramics at ambient temperature. doi: 10.1520/C1421-10
5. ASTM (2011) ASTM Standard, ASTM E1820 - 11 standard test method for measurement of fracture toughness. doi: 10.1520/E1820-11
6. ASTM (2002) ASTM Standard, ASTM C1211 - 02 standard test method for flexural strength of advanced ceramics at elevated temperatures
7. ASTM (2009) ASTM Standard, ASTM C 1499-09 standard test method for monotonic equibiaxial flexural strength of advanced ceramics at ambient temperature
8. Gladden JR, Li G, Adebisi R et al (2010) Phys Rev B 82:1. doi:10.1103/PhysRevB.82.045209
9. Duan B, Zhai P, Wen P, Zhang S (2012) Scr Mater 67:372. doi:10.1016/j.scriptamat.2012.05.028
10. Ueno K, Yamamoto A, Noguchi T et al (2004) J Alloy Compd 384:254
11. Ueno K, Yamamoto A, Noguchi T et al (2005) Mech Prop 388:118. doi:10.1016/j.jallcom.2004.07.005
12. Ueno K, Yamamoto A, Noguchi T et al (2005) J Alloy Compd 392:295. doi:10.1016/j.jallcom.2004.08.078
13. Ravi V, Firdosy S, Caillat T et al (2008) AIP Conf Proc 969:656. doi:10.1063/1.2845027
14. Firdosy SA, Ravi VA, Li B et al (2013) In: 11th international energy conversion engineering conference. doi:10.2514/6.2013-3929
15. Palmqvist S (1957) Jernkontorets Ann 141:300
16. Palmqvist S (1962) Arch Eisenhuettenwes 33:629
17. Palmqvist S (1963) Jernkontorets Ann 147:107
18. Lawn B, Wilshaw R (1975) J Mater Sci 10:1049. doi:10.1007/BF00823224
19. Lawn BR, Swain MV (1975) J Mater Sci 10:113. doi:10.1007/BF00541038

20. Lawn BR, Fuller ER (1975) J Mater Sci 10:2016. doi:10.1007/BF00557479
21. Evans AG (1979) In: Proceedings of the 11th National Symposium on fracture mechanics: Part II. ASTM, pp 112–135
22. Lankford J (1982) J Mater Sci Lett 1:493
23. Spiegler R, Schmauder S, Sigl LS (1990) J Hard Mater 1:147
24. Shetty DK, Wright IG, Mincer PN, Clauer AH (1985) J Mater Sci 20:1873. doi:10.1007/BF00555296
25. Niihara K (1983) J Mater Sci Lett 2:221
26. Gilman JJ (2009) Chemistry and physics of mechanical hardness. Wiley-Interscience, Hoboken
27. Evans AG, Charles EA (1976) J Am Ceram Soc 59:371. doi:10.1111/j.1151-2916.1976.tb10991.x
28. Zhao L-D, Zhang B-P, Li J-F et al (2008) J Alloy Compd 455:259. doi:10.1016/j.jallcom.2007.01.015
29. Ren F, Ni JE, Case ED, et al. (2007) MRS Proceedings. doi: 10.1557/PROC-1044-U04-04
30. May A, Fleurial J, Snyder G (2008) Phys Rev B 78:1. doi:10.1103/PhysRevB.78.125205
31. ASTM (2010) ASTM Standard, ASTM E122-10 standard test methods for determining average grain size
32. Ponton C, Rawlings R (1989) Mater Sci Technol 5:961
33. Cox WL, Steinfink H, Bradley WF (1965) Inorg Chem 5:318
34. ASTM (2008) ASTM Standard, ASTM C1327 - 08 standard test method for vickers indentation hardness of advanced ceramics. doi: 10.1520/C1327-08
35. Ren F, Case ED, Timm EJ, Schock HJ (2008) J Alloy Compd 455:340. doi:10.1016/j.jallcom.2007.01.086
36. Crocker AJ, Wilson M (1978) J Mater Sci 13:833. doi:10.1007/BF00570520
37. Rogl G, Rogl P (2011) Sci Adv Mater 3:517. doi:10.1166/sam.2011.1181
38. Kallel AC, Roux G, Martin CL (2013) Mater Sci Eng A 564:65
39. Pharr GM, Herbert EG, Gao Y (2010) Annu Rev Mater Res 40:271. doi:10.1146/annurev-matsci-070909-104456
40. Farges G, Degout D (1989) Thin Sol Films 181:365. doi:10.1016/0040-6090(89)90505-1
41. Sangwal K (2009) Cryst Res Technol 44:1019. doi:10.1002/crat.200900385
42. Gong J, Wu J, Guan Z (1999) J Eur Ceram Soc 19:2625
43. Shu JY, Fleck NA (1998) Int J Sol Struct 35:1363. doi:10.1016/S0020-7683(97)00112-1
44. Gerberich WW, Tymiak NI, Grunlan JC et al (2002) J Appl Mech 69:433. doi:10.1115/1.1469004
45. Gouldstone A, Chollacoop N, Dao M et al (2007) Acta Mater 55:4015. doi:10.1016/j.actamat.2006.08.044
46. Lawn BR, Marshall DB (1979) J Am Ceram Soc 62:347
47. Quinn GD (2007) Fractography of ceramics and glasses. National Institute of Standards and Technology, Washington, DC
48. Quinn GD, Bradt RC (2007) J Am Ceram Soc 680:673. doi:10.1111/j.1551-2916.2006.01482.x
49. Ponton C, Rawlings R (1989) Mater Sci Technol 5:865
50. Wiederhorn SM (1969) J Am Ceram Soc 1968:99
51. Ni JE, Case ED, Khabir KN et al (2010) Mater Sci Eng B 170:58. doi:10.1016/j.mseb.2010.02.026